

# Reactions of $[M(\text{Se}_4)_2]^{2-}$ Anions with $\text{TePEt}_3$ : $^{77}\text{Se}$ and $^{125}\text{Te}$ Spectra of $[\text{MTe}_n\text{Se}_{8-n}]^{2-}$ ( $\text{M} = \text{Zn, Cd, Hg}$ ; $n = 0-4$ ) and Preparation and Crystal Structure of $[\text{PPh}_4]_2[\text{Hg}(\text{Te}_2\text{Se}_2)_2]$

John C. Bollinger and James A. Ibers\*

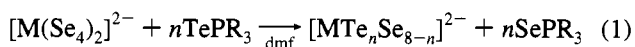
Department of Chemistry, Northwestern University, Evanston, Illinois 60208-3113

Received September 7, 1994<sup>⊗</sup>

$\text{TePEt}_3$  reacts quantitatively with  $[M(\text{Se}_4)_2]^{2-}$  anions ( $\text{M} = \text{Zn, Cd, Hg}$ ) in DMF. The ring-bound Se atoms are substituted by Te atoms in the  $\text{MSe}_4$  rings before the metal-bound Se atoms are. For  $n \leq 4$ , the reaction of  $n$  equiv of  $\text{TePEt}_3$  with 1 equiv of  $[M(\text{Se}_4)_2]^{2-}$  thus affords mixtures of  $[\text{MTe}_n\text{Se}_{8-n}]^{2-}$  anions, in which the Se atoms remain metal-bound. The pure isomer  $[\text{PPh}_4]_2[\text{Hg}(\text{Te}_2\text{Se}_2)_2]$  crystallizes in the tetragonal space group  $S_4^2-I4$  with four formula units in a unit cell of dimensions  $a = 21.174(5) \text{ \AA}$ ,  $c = 10.976(3) \text{ \AA}$ , and  $V = 4921(2) \text{ \AA}^3$  ( $T = 108 \text{ K}$ ). The values of the agreement indices  $R(F)$  and  $R_w(F^2)$  are 0.051 and 0.102, respectively. The  $[\text{PPh}_4]^+$  salts of  $[\text{Hg}(\text{Se}_4)_2]^{2-}$  and  $[\text{Hg}(\text{TeSe}_3)(\text{Se}_4)]^{2-}$  cocrystallize in a 0.42:0.58 ratio in the monoclinic space group  $C_{2h}^5-P2_1/n$  with eight formula units in a unit cell of dimensions  $a = 22.911(3) \text{ \AA}$ ,  $b = 20.161(4) \text{ \AA}$ ,  $c = 23.685(2) \text{ \AA}$ ,  $\beta = 118.65(1)^\circ$ , and  $V = 9601(2) \text{ \AA}^3$  ( $T = 108 \text{ K}$ ). The values of the final agreement indices are 0.078 and 0.153. The  $[\text{PPh}_4]^+$  salts of  $[\text{Hg}(\text{Se}_4)_2]^{2-}$ ,  $[\text{Hg}(\text{TeSe}_3)(\text{Se}_4)]^{2-}$ ,  $[\text{Hg}(\text{TeSe}_3)_2]^{2-}$ , and  $[\text{Hg}(\text{Te}_2\text{Se}_2)(\text{Se}_4)]^{2-}$  cocrystallize in a 0.05:0.39:0.43:0.13 ratio in the monoclinic space group  $C_{2h}^5-P2_1/c$  with eight formula units in a unit cell of dimensions  $a = 22.940(3) \text{ \AA}$ ,  $b = 20.220(2) \text{ \AA}$ ,  $c = 23.797(2) \text{ \AA}$ ,  $\beta = 118.50(1)^\circ$ , and  $V = 9701(2) \text{ \AA}^3$  ( $T = 108 \text{ K}$ ). The values of the agreement indices are 0.059 and 0.127. From the  $^{77}\text{Se}$  and  $^{125}\text{Te}$  NMR chemical shifts, which are sufficiently sensitive, it was possible with one exception to distinguish every unique chalcogen atom in every  $[\text{MTe}_n\text{Se}_{8-n}]^{2-}$  anion from every other one; these resonances are assigned and discussed.

## Introduction

Although considerable effort has been devoted to the preparation of new selenometalate complexes,<sup>1-4</sup> the reactivities of known complexes for the most part have not been studied. There is now considerable interest in tellurometalates,<sup>5-7</sup> so it is particularly apropos to investigate reactions that lead to the incorporation of tellurium into known selenometalate species.<sup>8</sup> Reactions of the following type fit that criterion:



In such reactions the compositions and structures of the chalcogenometalate products depend primarily on the number of equivalents of  $\text{TePR}_3$  used in the reaction, and a large number of compounds are readily accessible.

As both Se and Te have spin  $1/2$  isotopes— $^{77}\text{Se}$  and  $^{125}\text{Te}$ —NMR spectroscopy is a valuable tool for the characterization of chalcogenometalate products containing both Se and Te. Although  $^{77}\text{Se}$  NMR spectroscopy of selenometalate anions has been placed on relatively firm footing,<sup>4</sup> the spectral effects of replacing Se with other elements in such complexes are unknown. Some  $^{125}\text{Te}$  chemical shifts in tellurometalates have been measured,<sup>6,9,10</sup> but additional data are needed so that a  $^{125}\text{Te}$  NMR chemical shift scale can be established.

The synthesis and characterization of some  $[\text{MTe}_n\text{Se}_{8-n}]^{2-}$  anions was accomplished in accordance with eq 1 through the use of  $\text{TePEt}_3$ , and these results are reported here. It was possible with one exception to distinguish from their  $^{77}\text{Se}$  and  $^{125}\text{Te}$  chemical shifts every unique chalcogen atom in every  $[\text{MTe}_n\text{Se}_{8-n}]^{2-}$  anion from every other one, and these results are also reported.

## Experimental Section

The compounds  $[\text{PPh}_4]_2[\text{Hg}(\text{Se}_4)_2]$ ,  $[\text{NET}_4]_2[\text{Hg}(\text{Se}_4)_2]$ ,  $[\text{PPh}_4]_2[\text{Cd}(\text{Se}_4)_2]$ ,  $[\text{NET}_4]_2[\text{Cd}(\text{Se}_4)_2]$ ,  $[\text{PPh}_4]_2[\text{Zn}(\text{Se}_4)_2]$ ,  $[\text{NET}_4]_2[\text{Zn}(\text{Se}_4)_2]$ , and  $\text{TePEt}_3$  were prepared by literature methods.<sup>11,12</sup> Anhydrous DMF was purchased from Baxter Scientific Products and dried over molecular sieves. Toluene was purchased from Fisher Scientific, Springfield, NJ, and distilled from Na. Anhydrous  $\text{Et}_2\text{O}$  was purchased from Fisher Scientific and distilled from Na/benzophenone. All solvents were degassed before use. DMF- $d_7$  and 1.0 M  $\text{PEt}_3$  solution in THF were purchased from Aldrich Chemical Co., Milwaukee, WI, and used as received. Energy dispersive analysis by X-rays (EDAX) was performed with an Hitachi 570 scanning electron microscope equipped with an X-ray detector. Chemical microanalyses were performed by Oneida Research Services, Whitesboro, NY.

**Preparation of  $[\text{PPh}_4]_2[\text{Hg}(\text{Te}_2\text{Se}_2)_2]$  (1).**  $[\text{PPh}_4]_2[\text{Hg}(\text{Se}_4)_2]$  (378 mg, 0.25 mmol) and  $\text{TePEt}_3$  (246 mg, 1.00 mmol) were placed in separate Schlenk flasks. Because  $\text{TePEt}_3$  decomposes under vacuum by loss of  $\text{PEt}_3$ , the flask containing  $\text{TePEt}_3$  was filled with dry  $\text{N}_2$  by performing 10 quick cycles of evacuation and  $\text{N}_2$  refill. The flask containing  $[\text{PPh}_4]_2[\text{Hg}(\text{Se}_4)_2]$  was filled with  $\text{N}_2$  by the more normal process of two 15 min cycles of evacuation followed by  $\text{N}_2$  refills.  $[\text{PPh}_4]_2[\text{Hg}(\text{Se}_4)_2]$  was dissolved in DMF (10 mL) to afford a bright red solution, and  $\text{TePEt}_3$  was dissolved in DMF (1 mL) to afford a bright yellow solution. The  $\text{TePEt}_3$  solution was added dropwise via cannula to the stirred  $[\text{PPh}_4]_2[\text{Hg}(\text{Se}_4)_2]$  solution. The reaction mixture darkened with each drop of  $\text{TePEt}_3$  solution added, until the final

<sup>⊗</sup> Abstract published in *Advance ACS Abstracts*, March 1, 1995.

- (1) Kolis, J. W. *Coord. Chem. Rev.* **1990**, *105*, 195–219.
- (2) Krebs, B. *Angew. Chem., Int. Ed. Engl.* **1983**, *22*, 113–134.
- (3) Kanatzidis, M. G. *Comments Inorg. Chem.* **1990**, *10*, 161–195.
- (4) Ansari, M. A.; Ibers, J. A. *Coord. Chem. Rev.* **1990**, *100*, 223–266.
- (5) Ansari, M. A.; McConnachie, J. M.; Ibers, J. A. *Acc. Chem. Res.* **1993**, *26*, 574–578.
- (6) Roof, L. C.; Kolis, J. W. *Chem. Rev.* **1993**, *93*, 1037–1080.
- (7) Beck, J. *Angew. Chem., Int. Ed. Engl.* **1994**, *33*, 163–172.
- (8) McConnachie, J. M.; Bollinger, J. C.; Ibers, J. A. *Inorg. Chem.* **1993**, *32*, 3923–3927.
- (9) Björqvinnson, M.; Schrobilgen, G. J. *Inorg. Chem.* **1991**, *30*, 2540–2547.
- (10) Bollinger, J. C.; Roof, L. C.; Smith, D. M.; McConnachie, J. M.; Ibers, J. A. Unpublished results.

(11) Ansari, M. A.; Mahler, C. H.; Chorghade, G. S.; Lu, Y.-J.; Ibers, J. A. *Inorg. Chem.* **1990**, *29*, 3832–3839.

(12) Zingaro, R. A.; Steeves, B. H.; Irgolic, K. J. *Organomet. Chem.* **1965**, *4*, 320–323.

solution was a dark red-brown. A 1.0 M  $\text{PEt}_3$  solution in THF (0.2 mL) was added to the solution, and the mixture was then filtered into a fresh flask. Toluene (5 mL) was layered on top of the solution, and a large number of dark, needle-shaped crystals grew overnight. Additional crystals were obtained by layering more toluene on the mother liquor. Total yield: 302 mg, 71%. Semiquantitative elemental analysis by EDAX indicated approximately a 1:1 ratio of Se to Te. Anal. Calcd for  $\text{C}_{48}\text{H}_{40}\text{HgP}_2\text{Se}_4\text{Te}_4$ : C, 33.8; H, 2.36. Found: C, 33.6; H, 2.50.  $^{77}\text{Se}$  NMR (25 °C, DMF- $d_7$ ):  $\delta$  317, -213.

**Preparation of  $[\text{PPh}_4]_2[\text{HgTe}_{0.58}\text{Se}_{7.42}]$  (2).**  $[\text{PPh}_4]_2[\text{Hg}(\text{Se}_4)_2]$  (378 mg, 0.25 mmol) and  $\text{TePEt}_3$  (61 mg, 0.25 mmol) were added to separate Schlenk flasks and reacted as described for  $[\text{PPh}_4]_2[\text{Hg}(\text{Te}_2\text{Se}_2)_2]$ . The reaction mixture darkened slightly with each drop of  $\text{TePEt}_3$  solution added, but the final solution was not much darker than the original. This mixture was filtered into a fresh flask, and  $\text{Et}_2\text{O}$  (5.0 mL) was layered on top. Several very large, red, block-shaped crystals grew overnight. The mother liquor was very pale, so no attempt was made to obtain a second crop. Total yield: 304 mg, 79%. EDAX indicated a Se:Te ratio of about 11:1. The Se:Te ratio of 12.8:1 used here is derived from the X-ray crystallographic study where it is shown that several compounds cocrystallize to form these crystals. Anal. Calcd for  $\text{C}_{48}\text{H}_{40}\text{HgP}_2\text{Se}_{7.42}\text{Te}_{0.58}$ : C, 37.5; H, 2.62. Found: C, 37.1; H, 2.58.

**Preparation of  $[\text{PPh}_4]_2[\text{HgTe}_{1.52}\text{Se}_{6.48}]$  (3).**  $[\text{PPh}_4]_2[\text{Hg}(\text{Se}_4)_2]$  (378 mg, 0.25 mmol) and  $\text{TePEt}_3$  (123 mg, 0.50 mmol) were added to separate Schlenk flasks and reacted as described for  $[\text{PPh}_4]_2[\text{Hg}(\text{Te}_2\text{Se}_2)_2]$ . The reaction mixture darkened slightly with each drop of  $\text{TePEt}_3$  solution added, and the final solution was somewhat darker than the original. This mixture was filtered into a fresh flask, and  $\text{Et}_2\text{O}$  (5.0 mL) was layered on top. A large number of red, block-shaped crystals grew overnight. The mother liquor was very pale, so no attempt was made to obtain a second crop. Total yield: 295 mg, 74%. EDAX indicated a Se:Te ratio of about 3.5:1. The Se:Te ratio of 4.3:1 used here was derived from the X-ray crystallographic study; as for **2**, these crystals result from the cocrystallization of several compounds. Anal. Calcd for  $\text{C}_{48}\text{H}_{40}\text{HgP}_2\text{Se}_{6.48}\text{Te}_{1.52}$ : C, 36.4; H, 2.54. Found: C, 35.2; H, 2.49.

**Preparation of  $[\text{NEt}_4]^+$  Solutions of Mixed M/Te/Se Anions for NMR Spectroscopy.** Samples having  $M = \text{Zn, Cd, Hg}$  and  $n = 0.5, 1.0, 1.5, 2.0, 2.5, 3.0, 3.5,$  and  $4.0$  were all prepared in substantially the same way, so the preparation for  $M = \text{Hg}, n = 3.0$  is given as an example.  $[\text{NEt}_4]_2[\text{Hg}(\text{Se}_4)_2]$  (273 mg, 0.25 mmol) was added to a Schlenk flask under Ar in a drybox. The flask was then filled with dry  $\text{N}_2$  on a Schlenk line.  $\text{TePEt}_3$  (184 mg, 0.75 mmol) was measured into another Schlenk flask and placed under dry  $\text{N}_2$  by performing 10 quick cycles of evacuation and  $\text{N}_2$  refill.  $[\text{NEt}_4]_2[\text{Hg}(\text{Se}_4)_2]$  was dissolved in dry degassed DMF (2.5 mL) and DMF- $d_7$  (0.5 mL) was added.  $\text{TePEt}_3$  was dissolved in 0.5 mL of dry degassed DMF, and the solution was added dropwise via cannula to the stirred selenide solution. The  $\text{TePEt}_3$  flask and cannula were rinsed with more DMF (0.5 mL), and the rinse was added to the reaction mixture. Under  $\text{N}_2$  the resulting solution was filtered directly into a 10 mm NMR tube. The tube was closed under a flow of  $\text{N}_2$  with a plastic pressure cap and sealed with Teflon tape.

**Alternative Preparation of Mixed Hg/Te/Se Anions Solutions.** Reactions for  $n = 1, 2,$  and  $4$  were performed as indicated above. The solutions were filtered into fresh flasks, and toluene (2 mL) was layered on top. Crystals grew overnight, but they were poor in quality and mixed with noncrystalline precipitate. The crystals were manually separated from the precipitate under Ar in a glovebox. To each sample of crystals was added DMF- $d_7$  (0.5 mL). The materials did not completely dissolve. The saturated solutions were filtered into 5 mm NMR tubes, and the tubes were closed with septa. The tubes were then flame sealed.

**Structure of  $[\text{PPh}_4]_2[\text{Hg}(\text{Te}_2\text{Se}_2)_2]$  (1).** Preliminary film data obtained at 25 °C indicated that **1** crystallizes in Laue class  $4/m$  in a body-centered unit cell of dimensions  $a = 21.2 \text{ \AA}$  and  $c = 11.1 \text{ \AA}$ . The crystal used for Weissenberg photography was transferred to a Picker diffractometer equipped with a low-temperature device and operated by the program PCPS-1.<sup>13</sup> The final unit cell dimensions of  $a = 21.174(5) \text{ \AA}$  and  $c = 10.976(3) \text{ \AA}$  at 108 K were determined from

the setting angles of 47 well-centered reflections having  $18^\circ \leq 2\theta(\text{Mo K}\alpha_1) \leq 35^\circ$ .

Data having  $h, k \geq 0$  were collected for  $2\theta$  between 3 and  $55^\circ$ . The data were processed<sup>14</sup> and corrected for absorption effects.<sup>15</sup> As the data contain no systematic absences other than those attributable to body centering, the possible space groups are  $C_4^2-I4, S_6^2-I\bar{4},$  and  $C_4^2-I4/m$ . Four formula units per cell follow from consideration of atomic volumes. Neither the symmetry of the centrosymmetric space group  $I4/m$  nor that of the noncentrosymmetric space group  $I4$  can accommodate four anions of the expected structure in the unit cell, but the symmetry of space group  $I\bar{4}$  can. Furthermore, intensity statistics strongly suggested a noncentrosymmetric space group. Direct methods solutions were calculated in each of these three space groups as a precaution,<sup>16</sup> but only the solution in space group  $I\bar{4}$  was interpretable to afford the positions of the Hg, Se, Te, and P atoms.

Molecular graphics for analysis of intermediate crystallographic models and for publication were produced with the SHELXTL-PC program package.<sup>17</sup> Two crystallographically unique Hg atoms are each located on special positions of  $\bar{4}$  point symmetry, and all other atoms are on general positions. A slight disorder of the Te position in one of the  $\text{HgTe}_2\text{Se}_2$  five-membered rings was modeled by constraining the occupancy factors of the two sites to sum to 1.0. The positions of all C atoms were found in a difference electron density map. One of the phenyl rings is disordered over two slightly different orientations. Because of the proximity of some of the disordered C atoms to one another, successful anisotropic refinement of these atoms required that their displacement parameters be restrained to approximate an isotropic model. Hydrogen atoms were included at calculated positions and refined with the use of a riding model. All non-hydrogen atoms were refined anisotropically. The model converged to final values of  $R(F)$  ( $F_o^2 > 2\sigma(F_o^2)$ ) and  $R_w(F^2)$  (all data) of 0.051 and 0.102, respectively. Selected crystal and experimental details are listed in Table 1, heavy-atom coordinates and equivalent isotropic displacement parameters are listed in Table 2, and anion bond distances and angles are given in Table 3. Additional crystallographic details, C and H atom parameters, anisotropic displacement parameters, and complete bond distances and angles are provided in Tables S1–S4.<sup>18</sup> A view of the  $[\text{Hg}(\text{Te}_2\text{Se}_2)_2]^{2-}$  anion is presented in Figure 1.

**Structures of  $[\text{PPh}_4]_2[\text{HgTe}_{0.58}\text{Se}_{7.42}]$  (2) and  $[\text{PPh}_4]_2[\text{HgTe}_{1.52}\text{Se}_{6.48}]$  (3).** Data collection and structure solution and refinement proceeded as for **1**. The structure of **2** contains substantial disorder owing to the cocrystallization of nonidentical anions. A solution of **2** was determined by direct methods.<sup>16</sup> It contained positions for all of the atoms of the two unique anions and for all four P atoms. Two conformations for one of the chalcogenide rings in anion 1 were apparent in the structure solution. All ring atoms were initially assigned as Se. As groups, the atoms of each of the two disordered ring conformations were given common occupancy factors, which were refined as least-squares parameters with the sum constrained to be 1.0. The locations of the C atoms were determined from difference electron density maps. Once these had been refined, the bond distances and isotropic thermal displacement parameters of the erstwhile Se atoms were examined in order to identify the Te atoms among them. One Se position in each anion had unusually long bond distances and a comparatively small displacement parameter, so these positions were reassigned as Te. After refinement, however, the bond distances involving the Te atoms were too short, and the displacement parameters were large. Also, atom Te(27) was too close to an Se atom in one of the conformations of the disordered ring of anion 1. The model was therefore adjusted so that the ring positions in question contained Te atoms some of the time and Se atoms the rest of the time. The occupancy factors of the disordered Te/Se pairs were constrained to sum to 1.0, but the coordinates were allowed to refine separately. Additionally, atom Te-

(14) Waters, J. M.; Ibers, J. A. *Inorg. Chem.* **1977**, *16*, 3273–3277.

(15) de Meulenaer, J.; Tompa, H. *Acta Crystallogr.* **1965**, *19*, 1014–1018.

(16) Sheldrick, G. M. In *Crystallographic Computing 3*; Sheldrick, G. M., Krüger, C., Goddard, R., Eds.; Oxford University Press: London, 1985; pp 175–189.

(17) Sheldrick, G. M. *SHELXTL PC, Version 4.1. An integrated system for solving, refining, and displaying crystal structures from diffraction data*; Siemens Analytical X-Ray Instruments, Inc.: Madison, WI, 1990.

(18) Supplementary material.

**Table 1.** Crystal Data and Details of Structure Refinement for Compounds 1–3

compd	[PPh <sub>4</sub> ] <sub>2</sub> [Hg(Te <sub>2</sub> Se <sub>2</sub> ) <sub>2</sub> ] (1)	[PPh <sub>4</sub> ] <sub>2</sub> [HgTe <sub>0.58</sub> Se <sub>7.42</sub> ] (2)	[PPh <sub>4</sub> ] <sub>2</sub> [HgTe <sub>1.52</sub> Se <sub>6.48</sub> ] (3)
chem formula	C <sub>48</sub> H <sub>40</sub> HgP <sub>2</sub> Se <sub>4</sub> Te <sub>4</sub>	C <sub>48</sub> H <sub>40</sub> HgP <sub>2</sub> Se <sub>7.42</sub> Te <sub>0.58</sub>	C <sub>48</sub> H <sub>40</sub> HgP <sub>2</sub> Se <sub>6.48</sub> Te <sub>1.52</sub>
fw	1705.57	1539.27	1587.01
a, Å	21.174(5)	22.911(3)	22.940(3)
b, Å	21.174	20.161(4)	20.220(2)
c, Å	10.976(3)	23.685(2)	23.797(2)
β, deg	90	118.65(1)	118.50(1)
V, Å <sup>3</sup>	4921(2)	9601(2)	9701(2)
space group	S <sub>4</sub> <sup>2</sup> -I <sub>4</sub>	C <sub>2h</sub> <sup>5</sup> -P2 <sub>1</sub> /n	P2 <sub>1</sub> /n
Z	4	8	8
μ, cm <sup>-1</sup>	85	92	90
density (calc), g/cm <sup>3</sup>	2.302	2.131	2.173
T, K	108	108	108
R(F) <sup>a</sup> (F <sub>o</sub> <sup>2</sup> > 2σ(F <sub>o</sub> <sup>2</sup> ))	0.051	0.078	0.059
R <sub>w</sub> (F <sub>2</sub> ) <sup>b</sup> (all data)	0.102	0.153	0.127

$$^a R(F) = \sum ||F_o| - |F_c|| / \sum |F_o| \quad ^b R_w(F^2) = \{ \sum [w(F_o^2 - F_c^2)^2] / \sum wF_o^4 \}^{1/2}; w^{-1} = \sigma^2(F_o^2) + (0.04F_o^2)^2 \text{ for } F_o^2 \geq 0; w^{-1} = \sigma^2(F_o^2) \text{ for } F_o^2 < 0.$$

**Table 2.** Atomic Coordinates and Equivalent Isotropic Displacement Parameters (Å<sup>2</sup>) for the Heavy Atoms of [PPh<sub>4</sub>]<sub>2</sub>[Hg(Te<sub>2</sub>Se<sub>2</sub>)<sub>2</sub>]

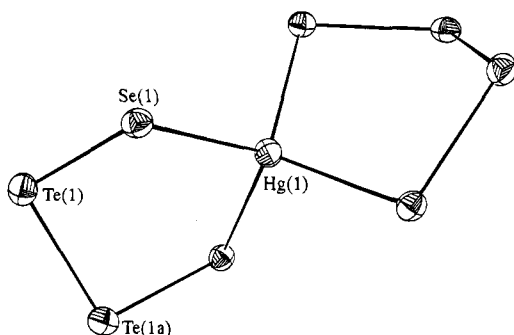
atom	x	y	z	U <sub>eq</sub> <sup>a</sup>
Hg(1)	0	1/2	1/4	0.0222(2)
Se(1)	0.10207(5)	0.49606(5)	0.10693(11)	0.0224(3)
Te(1)	0.05335(4)	0.46387(4)	-0.09270(7)	0.0255(2)
Hg(2)	0	0	0	0.0270(2)
Se(2)	0.03992(6)	0.09248(6)	-0.14538(11)	0.0295(3)
Te(21) <sup>b</sup>	0.05387(7)	0.03221(8)	-0.3334(2)	0.0302(5)
Te(22) <sup>b</sup>	-0.01106(7)	0.06227(7)	-0.34050(14)	0.0287(5)
P	0.24345(13)	0.33083(13)	0.2206(3)	0.0195(6)

<sup>a</sup> U<sub>eq</sub> is defined as one-third of the trace of the orthogonalized U<sub>ij</sub> tensor. <sup>b</sup> Occupancy 0.500(2).

**Table 3.** Selected Bond Lengths (Å) and Angles (deg) for [PPh<sub>4</sub>]<sub>2</sub>[Hg(Te<sub>2</sub>Se<sub>2</sub>)<sub>2</sub>]<sup>a</sup>

Hg(1)–Se(1)	2.673(1)	Se(2)–Te(21)	2.444(2)
Se(1)–Te(1)	2.516(2)	Se(2)–Te(22)	2.482(2)
Te(1)–Te(1) <sup>a</sup>	2.729(2)	Te(21)–Te(21) <sup>b</sup>	2.658(3)
Hg(2)–Se(2)	2.664(1)	Te(22)–Te(22) <sup>b</sup>	2.678(3)
Se(1) <sup>c</sup> –Hg(1)–Se(1)	110.19(3)	Se(2) <sup>b</sup> –Hg(2)–Se(2)	106.40(6)
Se(1)–Hg(1)–Se(1) <sup>a</sup>	108.04(5)	Te(21)–Se(2)–Hg(2)	99.23(6)
Te(1)–Se(1)–Hg(1)	100.87(4)	Te(22)–Se(2)–Hg(2)	100.92(6)
Se(1)–Te(1)–Te(1) <sup>a</sup>	100.81(3)	Se(2)–Te(21)–Te(21) <sup>b</sup>	99.45(6)
Se(2) <sup>d</sup> –Hg(2)–Se(2)	111.03(3)	Se(2)–Te(22)–Te(22) <sup>b</sup>	100.23(5)

<sup>a</sup> Symmetry transformations used to generate equivalent atoms: (a)  $-x, -y + 1, z$ ; (b)  $-x, -y, z$ ; (c)  $y - 1/2, -x + 1/2, -z + 1/2$ ; (d)  $y, -x, -z$ .

**Figure 1.** View of one  $[\text{Hg}(\text{Te}_2\text{Se}_2)_2]^{2-}$  anion, with the 50% probability thermal ellipsoids shown. The anion possesses crystallographically imposed symmetry  $\bar{4}$ . Bond lengths in the anion shown: Hg(1)–Se(1), 2.673(1) Å; Se(1)–Te(1), 2.516(2) Å; Te(1)–Te(1a), 2.729(2) Å.

(27) was linked to the disordered ring with which it had no close interactions so that they had a common occupancy factor. In order to stabilize the refinement, the displacement parameters of the corresponding Se and Te atoms were restrained to be equal, and chemically equivalent Se–Se and Se–Te bond distances throughout the structure were similarly, though less strongly, restrained to be equal. Hydrogen

atoms were included at calculated positions and refined with the use of a riding model. The anisotropic displacement parameters of the disordered Te/Se pairs and of all C atoms were restrained to approximate the isotropic model, and all non-hydrogen atoms were refined anisotropically. This model converged to values of  $R(F)$  of 0.078 ( $F_o^2 > 2\sigma(F_o^2)$ ) and  $R_w(F_o^2)$  of 0.153 (all data). It indicates that  $[\text{PPh}_4]_2[\text{Hg}(\text{Se}_4)_2]$  and  $[\text{PPh}_4]_2[\text{Hg}(\text{TeSe}_3)(\text{Se}_4)]$  cocrystallize in a 0.42:0.58 ratio. Additional crystallographic details are listed in Table S5, coordinates and equivalent isotropic displacement parameters for all atoms are listed in Table S6, anisotropic displacement parameters are listed in Table S7, and anion bond distances and angles are listed in Table S8.<sup>18</sup>

In the structure of **3** there is also some disorder, which we interpret as resulting from the cocrystallization of several compounds. Refinement proceeded along the lines described above for **2**. Atoms Se(16), Se(17), Se(36), Se(22), and Se(23) were modeled as partly Te and partly Se. In order to stabilize the refinement, the thermal displacement parameters of the corresponding Se and Te atoms were strongly restrained to be equal, and chemically equivalent Se–Se and Se–Te bond distances throughout the structure were less strongly restrained to be equal. The Te(22)–Te(23) bond has no analogue in the rest of the structure so that distance was restrained to a normal Te–Te distance of 2.76 Å. Hydrogen atoms were included at calculated positions and refined with the use of a riding model. The anisotropic displacement parameters of the disordered Te/Se pairs and of all C atoms were restrained to approximate the isotropic model, and all non-hydrogen atoms were refined anisotropically. This model converged to values of  $R(F)$  of 0.059 ( $F_o^2 > 2\sigma(F_o^2)$ ) and  $R_w(F_o^2)$  of 0.127 (all data). It indicates that  $[\text{PPh}_4]_2[\text{Hg}(\text{Se}_4)_2]$ ,  $[\text{PPh}_4]_2[\text{Hg}(\text{TeSe}_3)(\text{Se}_4)]$ ,  $[\text{PPh}_4]_2[\text{Hg}(\text{TeSe}_3)_2]$ , and  $[\text{PPh}_4]_2[\text{Hg}(\text{Te}_2\text{Se}_2)(\text{Se}_4)]$  cocrystallize in a 0.05:0.39:0.43:0.13 ratio. Owing to the complexity of the disorder, this ratio is semiquantitative, but it does provide an indication of the relative abundances of the various species. Additional crystallographic details are listed in Table S9, coordinates and equivalent displacement parameters for all atoms are listed in Table S10, anisotropic displacement parameters are listed in Table S11, and anion bond distances and angles are listed in Table S12.<sup>18</sup>

**Spectroscopy.** <sup>77</sup>Se and <sup>125</sup>Te NMR spectra of a solution prepared from crystals of  $[\text{PPh}_4]_2[\text{Hg}(\text{Te}_2\text{Se}_2)_2]$  (**1**) and of reaction mixtures of M/Te/Se anions prepared with  $[\text{NET}_4]^+$  cations as outlined above for M = Hg ( $n = 0.5, 1.0, 1.5, 2.0, 2.5, 3.0, 3.5, 4.0$ ) and M = Zn, Cd ( $n = 0.5, 2.0, 3.5$ ) were recorded with the use of a 400 MHz Varian Unity Plus NMR spectrometer equipped with a 10 mm broad-band probe, a variable-temperature apparatus, and a deuterium lock. <sup>77</sup>Se and <sup>125</sup>Te spectra of redissolved crystals of  $[\text{NET}_4]^+$  salts of mixed Hg/Te/Se anions, prepared in the alternative synthesis outlined above for  $n = 1, 2, 4$ , were recorded with the use of a Varian XLA-300 spectrometer equipped with a 5 mm broad-band probe, a variable-temperature apparatus, and a deuterium lock. Spectra of  $[\text{NET}_4]_2[\text{Hg}(\text{Te}_2\text{Se}_2)_2]$  were recorded at four temperatures between +20 and –40 °C to evaluate the possibility of dynamic processes occurring in solution. All other spectra were recorded at low temperature (–30 to –40 °C). Samples were prepared under N<sub>2</sub> or Ar in DMF/DMF-*d*<sub>7</sub>. All spectra were referenced to the external standards Ph<sub>2</sub>Se<sub>2</sub> at 460 ppm or Et<sub>2</sub>Te at 380 ppm.

## Results

**Syntheses.** Compounds of the type  $[\text{PPh}_4]_2[\text{HgTe}_n\text{Se}_{8-n}]$  are formed by reaction of  $[\text{PPh}_4]_2[\text{Hg}(\text{Se}_4)_2]$  with various amounts of  $\text{TePEt}_3$ . The compound  $[\text{PPh}_4]_2[\text{Hg}(\text{Te}_2\text{Se}_2)_2]$  (**1**) is obtained when 4 equiv of  $\text{TePEt}_3$  is used. When less than 4 equiv of  $\text{TePEt}_3$  is used, the  $[\text{PPh}_4]^+$  salts of various  $[\text{HgTe}_n\text{Se}_{8-n}]^{2-}$  anions form (**2**, **3**). Although most have not been isolated, all of the anions  $[\text{MTe}_n\text{Se}_{8-n}]^{2-}$  for  $\text{M} = \text{Zn}, \text{Cd}, \text{Hg}$  and  $n = 0-4$  have been detected by  $^{77}\text{Se}$  and  $^{125}\text{Te}$  NMR spectroscopy.

**Crystallographic Studies.** The structure of **1** consists of  $[\text{Hg}(\text{Te}_2\text{Se}_2)_2]^{2-}$  anions packed among the phenyl groups of  $[\text{PPh}_4]^+$  cations in channels parallel to the crystallographic  $c$  axis. There are four of these channels in the unit cell. The two unique Hg atoms reside on  $\bar{4}$  centers, so one-fourth of each anion is unique. Closest intermolecular  $\text{Te}\cdots\text{Te}$  contacts range from 3.956(2) Å for  $\text{Te}(1)\cdots\text{Te}(1')$  to 4.112(3) Å for  $\text{Te}(21)\cdots\text{Te}(21')$ , where for the disordered  $\text{HgTe}_2\text{Se}_2$  rings only interacting rings of the same conformation are considered. These distances are comparable to other  $\text{Te}\cdots\text{Te}$  nonbonding interactions, such as 4.144(2) Å in  $[\text{NET}_4]_3[\text{AuTe}_7]^{19}$  and 3.82-(1) Å in  $\text{HfTe}_2$ .<sup>20</sup> If any pair of adjacent anions were to have opposite ring conformations, then the intermolecular separation  $\text{Te}(21)\cdots\text{Te}(22')$  would be only 3.611(3) Å, not only too close to be considered noninteracting but also about 0.34 Å less than the three other intermolecular  $\text{Te}\cdots\text{Te}$  separations. A model in which all rings of all anions in each channel have the same conformation best satisfies the requirements of translational symmetry and local  $\bar{4}$  symmetry imposed by space group  $I\bar{4}$ . The excellent consistency among equivalent data supports such a model.

Bond lengths and displacement parameters in  $[\text{PPh}_4]_2[\text{Hg}(\text{Te}_2\text{Se}_2)_2]$  (**1**) are consistent with a model having only Se in the metal-bound positions and only Te in the ring-bound positions. The Hg–Se distances of 2.673(1) and 2.664(1) Å are normal and may be compared to average Hg–Se distances of 2.65(2) Å in  $[\text{PPh}_4]_2[\text{Hg}(\text{Se}_4)_2]^{11}$  and 2.650(4) Å in  $[\text{Na}(12\text{-crown-4})_2]_2[\text{Hg}(\text{Se}_4)_2]^{21}$ . The Te–Te distances of 2.658(3), 2.678(3), and 2.729(2) Å are reasonable single-bond distances, similar to Te–Te single-bond distances of 2.702(2) and 2.719(2) Å in  $[\text{NET}_4]_3[\text{AuTe}_7]^{19}$  and 2.682(2)–2.746(2) Å in  $[\text{PPh}_4]_2[\text{HgTe}_7]^{22}$  but somewhat shorter than the distances of 2.735(1)–2.774(1) Å in  $[\text{NET}_4]_4[\text{Ag}_2\text{Te}_{12}]^{23}$ . There are few known Te–Se bond distances, but the observed distances between 2.444(2) and 2.516(2) Å are comparable to those of 2.501(1) and 2.504(1) Å in  $[\text{K}(2,2,2\text{-crypt})]_2[\text{TeSe}_2]^{24}$  and 2.454(4)–2.465(4) Å in  $[\text{K}(2,2,2\text{-crypt})]_2[\text{TeSe}_3]^{24}$ . The  $\bar{4}$  point symmetry at the Hg centers would allow the coordination tetrahedra to be elongated, but the Se–Hg–Se angles in  $[\text{PPh}_4]_2[\text{Hg}(\text{Te}_2\text{Se}_2)_2]$  (**1**) range from 106.40(6) to 111.03(3)°, close to the ideal tetrahedral value. Hg–Se–Te and Se–Te–Te angles range from 99.23(6) to 100.92(6)° and average 100.25(6)°. The  $\text{HgTe}_2\text{Se}_2$  rings are constrained crystallographically to have symmetry 2; hence they have ideal half-chair conformations.<sup>25</sup>

Owing to the complexity of the disorder engendered by the cocrystallization of the  $[\text{PPh}_4]^+$  salts of mixtures of Hg/Te/Se anions, the structures of **2** and **3** are subject to large errors. But within those error limits the geometries of the ions are normal. Hg–Se distances range from 2.619(2) to 2.683(2) Å; Se–Se distances range from 2.250(3) to 2.437(4) Å; and Se–Te distances range from 2.466(6) to 2.560(7) Å. Hg coordination geometries are distorted tetrahedral, with angles ranging from 90.95(6) to 125.93(6)°. Angles around Se and Te range from 92.1(10) to 117.5(7)° (Tables S8 and S12).<sup>18</sup>

**Spectroscopy.** No  $^{77}\text{Se}$  or  $^{125}\text{Te}$  NMR spectra for solutions of **1–3** could be obtained on the XLA-300 spectrometer, probably because the  $[\text{PPh}_4]^+$  salts are not sufficiently soluble. In order to obtain spectra, solutions of the  $[\text{NET}_4]^+$  salts of the same anions were prepared from crystals, as described above. The  $^{77}\text{Se}$  NMR spectra of these samples contain numerous peaks, some near the known resonances for the  $[\text{Hg}(\text{Se}_4)_2]^{2-}$  anion and some relatively far away. However, each of the peaks in each of the three spectra falls into one of four narrow ranges near 595, 330, 75, and –210 ppm. Spectra measured at –30 °C contain the same peaks in essentially the same intensity ratios as those measured at 25 °C, but the peaks in spectra obtained at –30 °C are better resolved from each other. The  $^{125}\text{Te}$  NMR spectrum measured at –30 °C for crystals of nominal composition  $[\text{NET}_4]_2[\text{Hg}(\text{Te}_2\text{Se}_2)_2]$  contains only a broad hump centered near 550 ppm, but the spectrum for crystals of nominal composition  $[\text{NET}_4]_2[\text{HgTe}_2\text{Se}_6]$  contains intense, albeit broad, peaks at approximately 1050 and 570 ppm. With the use of the 400 MHz Unity Plus spectrometer, we recorded at 25 °C the  $^{77}\text{Se}$  NMR spectrum of a sample of  $[\text{PPh}_4]_2[\text{Hg}(\text{Te}_2\text{Se}_2)_2]$  (**1**) prepared by dissolving crystals in DMF/DMF- $d_7$  and of a reaction mixture containing  $[\text{NET}_4]_2[\text{Hg}(\text{Se}_4)_2]$  and 4 equiv of  $\text{TePEt}_3$ . The resonances from the spectrum of **1** ( $\delta$  317, –213) also appear in the spectrum of the reaction mixture, although the latter contains additional, minor resonances as well. The anion of **1** has only one type of Se, and therefore its  $^{77}\text{Se}$  spectrum should contain only one resonance. In fact, the resonance at  $\delta$  –213 in the spectrum of **1** is substantially more intense than the resonance at  $\delta$  317. Probably the crystals from which the sample was prepared included some of  $[\text{PPh}_4]_2[\text{HgTe}_3\text{Se}_5]$ . The spectrum of the reaction mixture had a much better signal-to-noise ratio than did that of **1**, and a spectrum obtained at –30 °C for the reaction mixture was even more intense and better resolved. All further samples were therefore prepared from reaction mixtures of  $[\text{NET}_4]^+$  salts, and all further spectra were recorded at low temperature. There are neither changes in line widths nor the appearance or disappearance of peaks with changes in temperature that would point to any dynamic processes occurring in solution.  $^{77}\text{Se}$  spectra for the reaction mixtures containing  $[\text{NET}_4]_2[\text{Hg}(\text{Se}_4)_2]$  and 1 or 2.5 equiv of  $\text{TePEt}_3$  are given as examples in Figures 2 and 3, respectively.

For a particular metal M there are five structurally different anions that can be generated by replacing some or all of the ring-bound Se atoms of the  $[\text{M}(\text{Se}_4)_2]^{2-}$  anion with Te atoms. Each of these anions has between one and five magnetically distinct types of Se atoms and either one or two magnetically distinct types of Te atoms, so it is necessary to introduce a notation to designate each type of Se atom in each compound. Chart 1 shows representations of the five selenotelluride compounds and the parent selenide, with the atoms labeled according to the notation devised here. Each Se atom is given a label consisting of the number of Te atoms in the anion (but see below), M for metal-bound or R for ring-bound, and S for

(19) Ansari, M. A.; Bollinger, J. C.; Ibers, J. A. *J. Am. Chem. Soc.* **1993**, *115*, 3838–3839.

(20) Lévy, F., Ed. *Crystallography and Crystal Chemistry of Materials with Layered Structures*; Physics and Chemistry of Materials with Layered Structures 2; D. Reidel: Dordrecht, Holland, 1976.

(21) Ahle, A.; Dehnicke, K.; Maczek, K.; Fenske, D. *Z. Anorg. Allg. Chem.* **1993**, *619*, 1699–1703.

(22) McConnachie, J. M.; Ansari, M. A.; Bollinger, J. C.; Salm, R. J.; Ibers, J. A. *Inorg. Chem.* **1993**, *32*, 3201–3202.

(23) Ansari, M. A.; Bollinger, J. C.; Ibers, J. A. *Inorg. Chem.* **1993**, *32*, 1746–1748.

(24) Björgvinsson, M.; Sawyer, J. F.; Schrobilgen, G. J. *Inorg. Chem.* **1991**, *30*, 4238–4245.

(25) Banda, R. M. H.; Cusick, J.; Scudder, M. L.; Craig, D. C.; Dance, I. G. *Polyhedron* **1989**, *8*, 1995–1998.

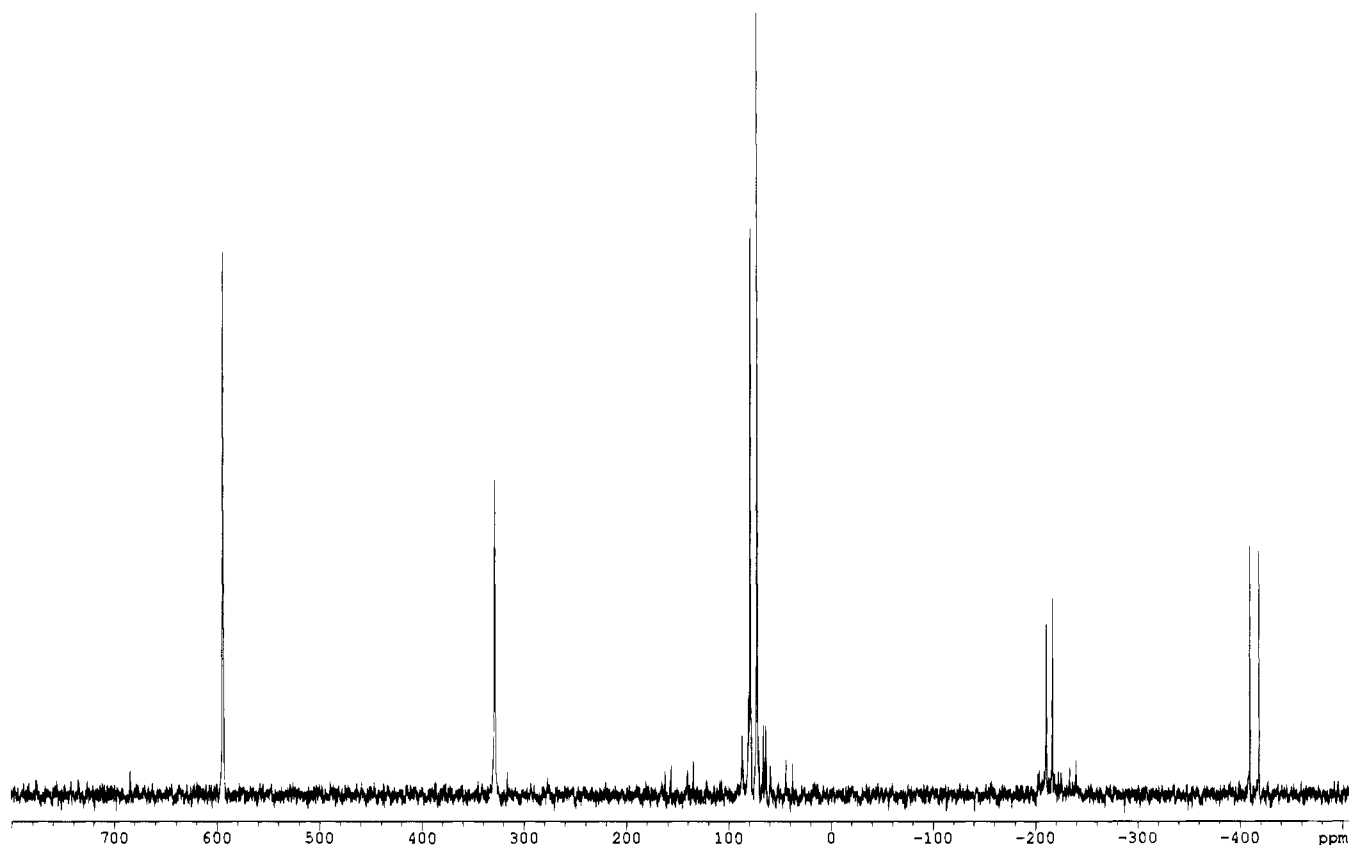


**Figure 2.**  $^{77}\text{Se}$  spectrum of the reaction mixture  $[\text{NEt}_4]_2[\text{Hg}(\text{Se}_4)_2] + \text{TePEt}_3$  (1:1). The doublet at  $\delta -415$  arises from  $\text{SePEt}_3$ .

those atoms bound to ring Se or T for those atoms bound to ring Te. Where further distinction is necessary, the atom type corresponding to the greater number of Se atoms is designated a, and the other b. There are two isomers of composition  $[\text{MTe}_2\text{Se}_6]^{2-}$ , so the isomer with two  $\text{TeSe}_3^{2-}$  ligands is labeled  $2\alpha$  and the one with one  $\text{Se}_4^{2-}$  ligand and one  $\text{Te}_2\text{Se}_2^{2-}$  ligand is labeled  $2\beta$ . Except for  $[\text{MTe}_3\text{Se}_5]^{2-}$ , there is only one type of Te in each anion, so the Te atoms are labeled only with the total number Te atoms in the complex. For  $[\text{MTe}_3\text{Se}_5]^{2-}$  the two equivalent Te atoms are designated 3a and the unique Te atom is designated 3b.

For each metal, Se resonances are observed in four well-separated, relatively narrow regions. The resonances in each region should correspond to a group of Se atoms each having bonds to the same combination of elements. These groups of Se atoms are classified above (MS, MT, RS, RT), so each class can be assigned to a spectral region. From the known resonances of the  $[M(\text{Se}_4)_2]^{2-}$  anions, the group of resonances at lowest field can be assigned to the RS class and the group at second-highest field can be assigned to the MS class. We assume that the relative order of the RT and MT classes is the same as that of their RS and MS counterparts and assign the groups at second lowest field to the RT class and the groups at highest field to the MT class. These assignments are supported by consistent interpretations of the spectra. For each metal the Te resonances fall into two groups. The downfield group of resonances appears with even the least amount of  $\text{TePEt}_3$  and disappears as the amount of Te approaches 4 equiv, so this group is assigned to Te atoms bound to two Se atoms. The other group of Te resonances appears later and continues to grow stronger as more Te is added, so it is assigned to Te atoms bound to Se and Te. According to these assignments, in every case Se and Te atoms bound to Te resonate upfield from their Se-bound analogues.

Within each group of resonances for each metal, peaks were assigned to particular Se or Te atoms from an analysis of the variation in peak intensity with the amount of  $\text{TePEt}_3$  in the reaction. Figure 4 contains an expanded view of the MS regions of the spectra in Figures 2 and 3; the decrease in the OMS resonance and the increases in the 1MS and  $2\alpha\text{MS}$  resonances are clearly visible. Multiple resonances from the same anions were distinguished by relative intensities. In the Hg system, no unique signal can be attributed to the Se(1MSb) atoms. In the Zn and Cd systems, however, the Se(1MSb) center resonates between the Se(1MSa) and Se(OMS) centers, so it is possible that in the Hg system the Se(1MSb) atoms coincidentally resonate at the same frequency as the Se(OMS) atoms. Otherwise, the ordering of both Se and Te resonance frequencies is identical for the three metal systems, and a resonance is assigned to every magnetically distinct atom. Resonances of the  $2\alpha\text{MS}$  and  $2\alpha\text{MT}$  atoms are between 3 and 8 times more intense than those of the  $2\beta\text{MS}$  and  $2\beta\text{MT}$  atoms, respectively, in those spectra where both appear. Thus in all three metal systems the  $[\text{M}(\text{SeTeSeSe})_2]^{2-}$  anion is formed preferentially to the  $[\text{M}(\text{SeTeTeSe})(\text{Se}_4)]^{2-}$  anion. Figure 5 contains an enlarged view of the MT region of Figure 2 showing the difference between the  $2\alpha\text{MT}$  and  $2\beta\text{MT}$  resonances. The  $^{77}\text{Se}$  resonances from these systems are presented in Table 4 and the  $^{125}\text{Te}$  resonances are presented in Table 5. The resonance positions are reported to tenths of a ppm in the tables in order to distinguish among  $^{125}\text{Te}$  resonances and among  $^{77}\text{Se}$  resonances of the RS and RT classes, each of which span only a few ppm (Figures 6 and 7), although  $^{77}\text{Se}$  resonances of the MS and MT classes span larger ranges, up to almost 40 ppm (Figures 4 and 5). The accuracy of these measurements is only slightly exaggerated, however. The differences among the breadths of the  $^{77}\text{Se}$  spectral ranges are reasonable, as the effect of a substitution on NMR frequencies depends on the number of

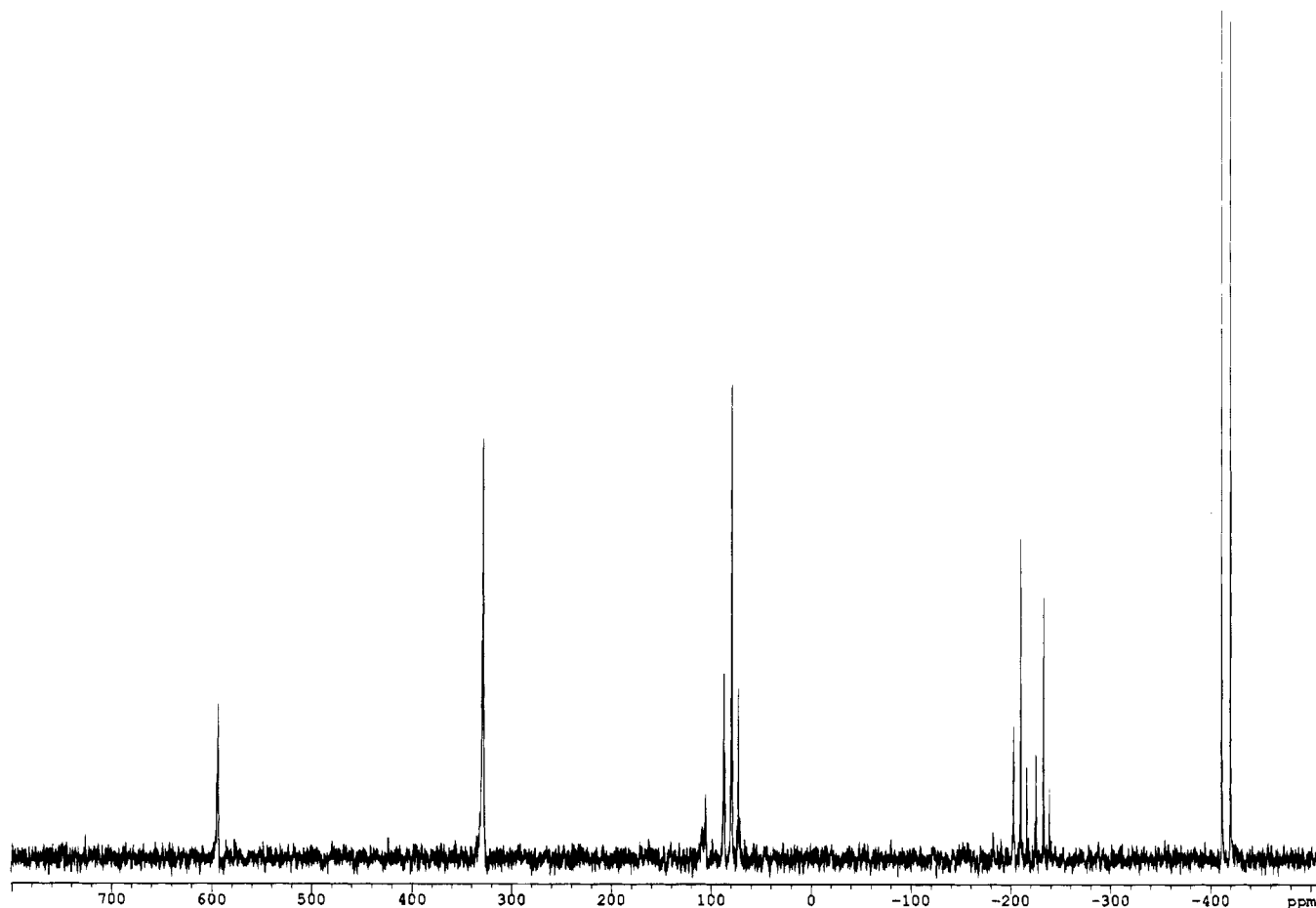
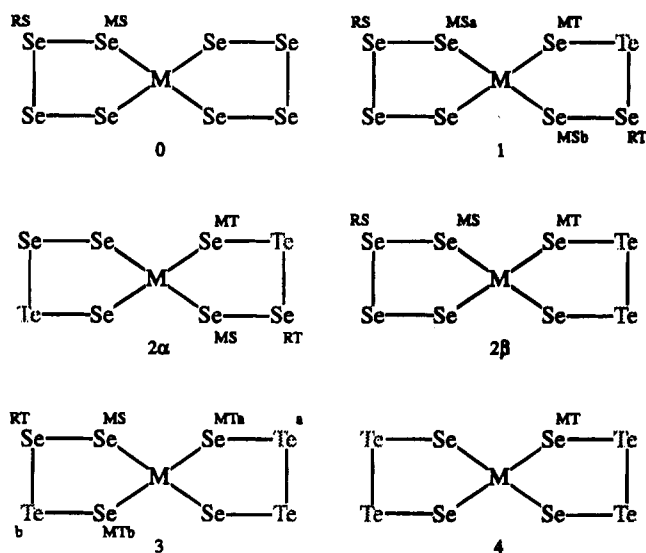


Figure 3.  $^{77}\text{Se}$  spectrum of the reaction mixture  $[\text{NEt}_4]_2[\text{Hg}(\text{Se}_4)_2] + \text{TePEt}_3$  (1:2.5). The doublet at  $\delta -415$  arises from  $\text{SePEt}_3$ .

Chart 1. Representation of the  $[\text{MTe}_n\text{Se}_{8-n}]^{2-}$  Anions,  $n = 0-4$ , Showing the Labeling Scheme for Se and Te Atoms



bonds separating the resonating atom from the site of substitution. The differences among resonances of the RS and RT classes result from substitutions four bonds away, whereas differences among the resonances of the MS and MT classes correspond to substitutions two or three bonds away. The Te resonances all arise from ring-bound atoms, and are close together in each class, just as the Se atoms are in classes RS and RT. Analysis of the changes in both Se and Te resonance frequencies as Te is substituted for Se reveals several trends: (a) substitution of an adjacent Se atom by Te results in a strong

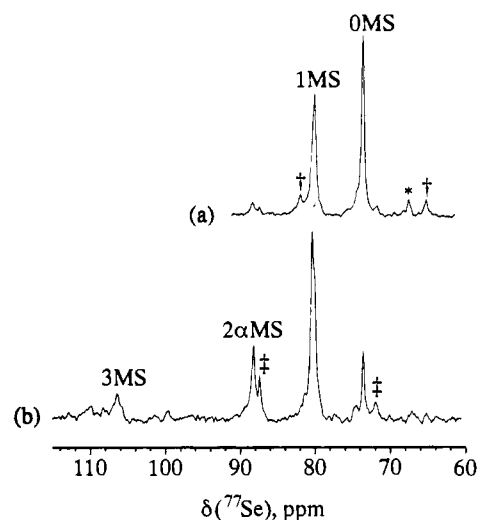
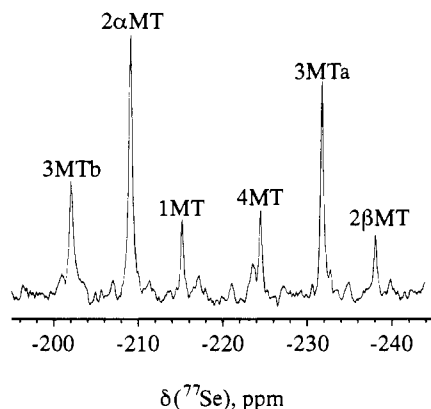


Figure 4. Expanded view of the MS regions of (a) Figure 2 and (b) Figure 3. The † and ‡ symbols designate satellite peaks arising from Se–Hg coupling to Se atoms OMS and 1MS, respectively. The \* indicates a resonance due to an impurity that is also present in the selenometalate starting material.

upfield shift of the resonance; (b) substitution of an Se atom in the opposite ring results in a moderate-to-small downfield shift; (c) substitution of an Se atom two bonds away in the same ring results in a downfield shift for MS atoms but an upfield shift for MT atoms.

$^{77}\text{Se}$  resonances in the RS and MS classes are similar to those for the appropriate parent selenides (Table 4). These, in turn, may be compared to the chemical shifts for the free  $\text{Se}_4^{2-}$  anion



**Figure 5.** Expanded view of the MT region of Figure 3. The difference between the intensities of the  $2\alpha\text{MT}$  and  $2\beta\text{MT}$  resonances arises from differing concentrations of the corresponding anions.

**Table 4.**  $^{77}\text{Se}$  NMR Resonances (ppm) for the  $[\text{MTe}_n\text{Se}_{8-n}]^{2-}$  Anions ( $M = \text{Zn, Cd, Hg; } n = 0-4$ )<sup>a</sup>

atom <sup>b</sup>	metal, M		
	Zn	Cd	Hg
ORS	599.1	607.2	594.1
IRS	600.2	607.6	594.5
$2\beta\text{RS}$	602.1	608.3	595.5
1RT	309.2	324.7	328.6
$2\alpha\text{RT}$	310.5	325.8	329.2
3RT	312.8	326.6	330.3
OMS	123.6	58.2	73.5
1MSa	129.6	63.0	80.4
1MSb	125.9	61.1	73.5
$2\alpha\text{MS}$	132.2	66.4	88.4
$2\beta\text{MS}$	137.1	69.4	108.4
3MS	140.4	73.0	106.7
1MT	-181.2	-257.6	-215.4
$2\alpha\text{MT}$	-175.6	-252.7	-209.0
$2\beta\text{MT}$	-202.9	-280.0	-238.2
3MTa	-196.1	-274.9	-231.6
3MTb	-169.0	-246.6	-201.8
4MT	-190.2	-269.0	-224.2

<sup>a</sup> The cation is  $[\text{NEt}_4]^+$ ; the temperature is  $-30^\circ\text{C}$ ; the solvent is DMF. <sup>b</sup> See Chart 1 for notation.

**Table 5.**  $^{125}\text{Te}$  NMR Resonances (ppm) for the  $[\text{MTe}_n\text{Se}_{8-n}]^{2-}$  Anions ( $M = \text{Zn, Cd, Hg; } n = 0-4$ )<sup>a</sup>

atom <sup>b</sup>	metal, M		
	Zn	Cd	Hg
1	1044.3	1047.6	1037.3
$2\alpha$	1045.6	1048.4	1037.9
3b	1047.7	1049.1	1039.7
$2\beta$	530.2	545.9	555.2
3a	532.3	546.5	557.0
4	535.3	547.5	558.4

<sup>a</sup> The cation is  $[\text{NEt}_4]^+$ ; the temperature is  $-30^\circ\text{C}$ ; the solvent is DMF. <sup>b</sup> See Chart 1 for notation.

(Table 6). In particular, the internal Se atoms of  $\text{Se}_4^{2-}$  resonate at 581 ppm (DMF/EtOH, 65/35),<sup>26</sup> close to the resonances of 594.1–608.3 ppm observed for the RS class. The resonances of Se atoms  $\beta$  to the ends of  $\text{Se}_3^{2-}$  and  $\text{Se}_6^{2-}$  chains also fall in the same region (Table 6).<sup>26</sup> A strong solvent proticity effect on  $^{77}\text{Se}$  resonance positions, an effect correlated with negative charge density on the affected atom, has been described.<sup>26</sup> This effect may be used to explain why the  $^{77}\text{Se}$  resonances, especially those of terminal Se atoms, observed for  $\text{Se}_3^{2-}$  and

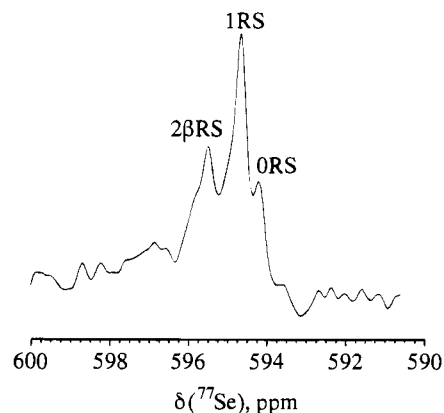


**Figure 6.** Expanded view of the RS region of Figure 3. The three resonances are all within a range of just 3 ppm.

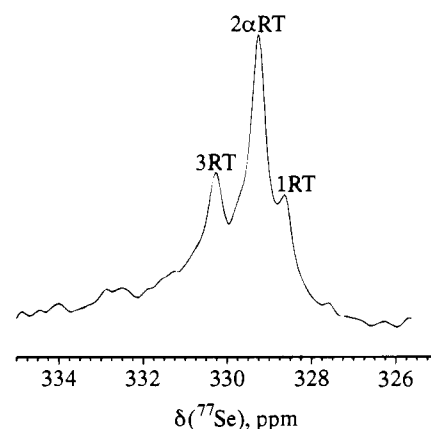


**Figure 7.** Expanded view of the RT region of Figure 3. As in Figure 6, the three resonances are within a range of about 3 ppm.

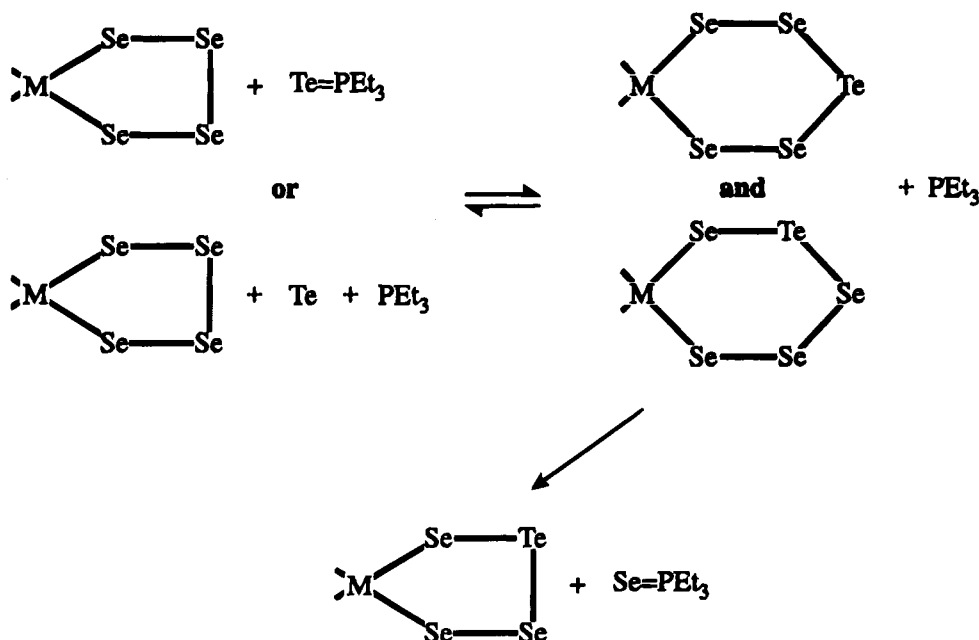
**Table 6.**  $^{77}\text{Se}$  and  $^{125}\text{Te}$  NMR Chemical Shifts for Several Known Anions

anion	solvent	temp, °C	$\delta(^{77}\text{Se}), \text{ppm}^a$	$\delta(^{125}\text{Te}), \text{ppm}$	ref
$\text{HSe}^-$	DMF/EtOH	27	-475		26
$\text{Se}_3^{2-}$	DMF/EtOH	-35	193 ( $\text{Se}_i$ ) 214 ( $\text{Se}_\beta$ )		26
$\text{Se}_4^{2-}$	DMF/EtOH	-35	256 ( $\text{Se}_i$ ) 581 ( $\text{Se}_\beta$ )		26
$\text{Se}_4^{2-}$	$\text{NH}_3(\text{l})$	-75	321 ( $\text{Se}_i$ ) 608 ( $\text{Se}_\beta$ )		9
$\text{Se}_5^{2-}$	DMF/EtOH	-35	354 ( $\text{Se}_i$ ) 570, 868 ( $\text{Se}_\beta$ )		26
$\text{Se}_6^{2-}$	DMF/EtOH	-35	404 ( $\text{Se}_i$ ) 636, 807 ( $\text{Se}_\beta$ )		26
$\text{HTe}^-$	EtOH	24		-1095	9
$\text{Te}_3^{2-}$	en	24		-298 ( $\text{Te}_i$ ) <sup>a</sup> -372 ( $\text{Te}_\beta$ ) <sup>a</sup>	9
$\text{Te}_2\text{Se}_2^{2-}$	en	53	-92	536	9
$\text{Te}_2\text{Se}_3^{2-}$	en	24	468	1087	9
$\text{Te}_2\text{Se}_2^{2-}$	en	24	-55	666	9

<sup>a</sup> The "t" subscript denotes terminal atoms, and the "b" subscript denotes bridging atoms.

$\text{Se}_4^{2-}$  in en<sup>9</sup> do not agree well with those observed for the same anions in DMF/EtOH.<sup>26</sup> The present  $[\text{MTe}_n\text{Se}_{8-n}]^{2-}$  spectra were all recorded from solutions with DMF as the solvent, and the observed resonances are more comparable to others observed from a similar solvent system.<sup>26</sup> A strong upfield shift (ca. 375 ppm) of the  $^{77}\text{Se}$  resonance for the (terminal) Se atoms of  $\text{Te}_2\text{Se}_2^{2-}$  with respect to the  $^{77}\text{Se}$  resonances for the corresponding atoms in  $\text{Se}_4^{2-}$  has been reported,<sup>9</sup> and a similar shift (ca. 300 ppm) is observed between the MS and MT classes in the  $[\text{MTe}_n\text{Se}_{8-n}]^{2-}$  anions.

Scheme 1

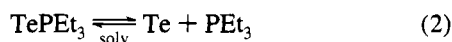


There are few comparisons to be made with the  $^{125}\text{Te}$  resonances observed for the  $[\text{MTe}_n\text{Se}_{8-n}]^{2-}$  anions (Table 6). The  $^{125}\text{Te}$  resonance for  $[\text{Te}_2\text{Se}_2]^{2-}$  in en occurs at 666 ppm,<sup>9</sup> as compared to the resonances of 530.2–558.4 ppm we observe for the same ligand complexed to Zn, Cd, and Hg. Whereas in solution the straight-chain  $[\text{TeSe}_3]^{2-}$  anion apparently does not exist, the pyramidal  $[\text{TeSe}_3]^{2-}$  anion exists in en and its  $^{125}\text{Te}$  resonance is found at 1087 ppm,<sup>9</sup> near the resonances of 1037.3–1049.1 ppm observed for  $\text{MTeSe}_3$  rings.

Cd and Hg have isotopes with spin  $1/2$ , and Se–M coupling is observed for the more intense MS and MT resonances in these systems. Se–Se and Se–Te couplings are not routinely observed under our experimental conditions, but in the spectrum of  $[\text{NEt}_4]_2[\text{Zn}(\text{Se}_4)_2] + \text{TePEt}_3$  (1:1) we observed a coupling of 75 Hz between Se atoms Se(ORS) and Se(OMS), and in the spectrum of  $[\text{NEt}_4]_2[\text{Zn}(\text{Se}_4)_2] + \text{TePEt}_3$  (1:3.5) we observed a coupling of 510 Hz between atoms Se(4MT) and Te(4). More than the usual number of transients were collected for those spectra, and observation of the weak satellite peaks arising from Se–Se and Se–Te coupling is simplified in the Zn system because of the absence of Se–Zn satellite peaks.

### Discussion

Although data on bond energies for selenometalates and tellurometalates are sorely lacking, we attribute the driving force for these substitution reactions to the formation of a fairly strong Se=P bond; the expected large difference between Te=P and Se=P bond strengths outweighs expected small differences among Se–Se, Se–Te, and Te–Te bond strengths. Indeed, the Te=P bond in  $\text{TePEt}_3$  is weak, as the following equilibrium is established in solution:<sup>12</sup>



The fact that  $\text{SePEt}_3$  does not dissociate in solution underscores the relative strength of the Se=P bond compared to the corresponding Te=P bond. In every case studied,  $^{31}\text{P}$  NMR analysis of the product mixtures showed that  $\text{TePEt}_3$  had reacted quantitatively with  $[\text{Hg}(\text{Se}_4)_2]^{2-}$  to form  $\text{SePEt}_3$ .<sup>27</sup> If  $\text{SePEt}_3$  were able to react with the Te in the metal-containing product,

then some  $\text{TePEt}_3$  would also have been seen. Indeed, in control experiments we found that  $\text{TePEt}_3$  reacted quantitatively with Se powder to produce  $\text{SePEt}_3$  and Te powder.<sup>27</sup>

The nature of the driving force notwithstanding, kinetics, rather than thermodynamics, appear to govern the nature of the products. Mixtures of selenometalate species are produced, but there is no evidence from NMR spectroscopy for any interconversions among these species. Furthermore, both NMR spectroscopy and crystallography show that, of the two isomers of the  $[\text{MTe}_2\text{Se}_6]^{2-}$  anion, the isomer having the Te atoms in opposite rings is produced preferentially. Entropic arguments would predict an approximately equal mixture, and perturbations owing to enthalpic differences between isomers should be small, so the observations are not explained by a thermodynamic argument. On the other hand, a kinetic argument can explain why formation of two  $\text{M}(\text{TeSe}_3)$  rings is favored over formation of an  $\text{M}(\text{Te}_2\text{Se}_2)$  ring. Consider the reaction pathway shown in Scheme 1. It is unclear whether the reactive Te species is  $\text{TePEt}_3$  or atomically dispersed Te, but it inserts Te into an Se–Se (or Se–Te) bond. There is then necessarily free  $\text{PEt}_3$  available, which can remove either Se or Te from the ring. Removal of Te results in re-formation of the starting materials and continuation of the reaction, but removal of Se results in formation of unreactive  $\text{SePEt}_3$ . Substitution into M–Se bonds should be less favorable than substitution into Se–Se or Se–Te bonds, both because M–Se bonds are more polar and hence stronger and because the second ring partially blocks access to the area near the metal. Indeed, substitution at the metal-bound sites is observed only when sufficient  $\text{TePEt}_3$  is used so that all the ring-bound Se atoms are substituted by Te. This reaction pathway also provides an explanation for the predominance of the  $[\text{MTe}_2\text{Se}_6]^{2-}$  isomer having the Te atoms in opposite rings (2 $\alpha$ , Chart 1). The intermediate leading to formation of an  $\text{M}(\text{Te}_2\text{Se}_2)$  ring contains two reactive Te atoms and only one reactive Se atom. To a first approximation, then, this intermediate is twice as likely to lose Te and thus regenerate an  $\text{M}(\text{TeSe}_3)$  ring as it is to lose Se to generate an  $\text{M}(\text{Te}_2\text{Se}_2)$  ring. By a parallel argument, the intermediate leading to initial formation of an  $\text{M}(\text{TeSe}_3)$  species is more likely to generate  $\text{M}(\text{TeSe}_3)$  than to regenerate  $\text{M}(\text{Se}_4)$ . Therefore an isolated  $[\text{M}(\text{TeSe}_3)(\text{Se}_4)]^{2-}$  anion is more likely to react to form  $[\text{M}(\text{TeSe}_3)_2]^{2-}$

(27) Salm, R. J.; Ibers, J. A. Unpublished work.



than to form  $[M(\text{Te}_2\text{Se}_2)(\text{Se}_4)]^{2-}$ , and the former complex predominates in the product mixtures.

$\text{PEt}_3$  added to the reaction solution for compound **1** prevents the precipitation of a dark powder, presumably elemental Te. The  $\text{PEt}_3$  does not appear to affect the nature of the isolated product, as crystals obtained from preparations identical to the one reported above, save for the exclusion of  $\text{PEt}_3$ , were determined by EDAX and a unit cell determination to be **1**. Presumably  $\text{PEt}_3$  solubilizes the Te precipitate by forming  $\text{TePEt}_3$ .  $\text{PEt}_3$  cannot be used in reactions with fewer than 4 equiv of  $\text{TePEt}_3$ , however, for then large amounts of insoluble red-purple precipitate form. In these cases the phosphine probably reacts with the remaining ring-bound Se atoms of the products. As the reaction solutions containing only Te in the ring-bound positions do not exhibit this behavior, it appears that the reactivity of ring-bound Te atoms is markedly less than that of ring-bound Se atoms.

Selenotelluride anions are not new, but their coordination to metals appears to be. Na and K salts of the  $[\text{TeSe}_3]^{2-}$  anion were first prepared by solid-state techniques.<sup>28</sup> Since then, a series of  $[\text{Te}_m\text{Se}_n]^{2-}$  anions has been characterized by NMR spectroscopy,<sup>9</sup> and some of these by X-ray crystallographic methods as well.<sup>24</sup> These studies show the structure of the

uncoordinated  $[\text{TeSe}_3]^{2-}$  anion to be trigonal pyramidal,<sup>9,24</sup> with Te as the central atom, whereas we find the coordinated  $[\text{TeSe}_3]^{2-}$  ligand to be straight-chain in the solid state. The reaction scheme proposed above must lead initially to formation of a species in solution possessing a straight-chain  $[\text{TeSe}_3]^{2-}$  ligand; conceivably this species could (but did not) rearrange prior to crystallization. Conversely, it is possible that any isolated pyramidal  $[\text{TeSe}_3]^{2-}$  species present in solution could rearrange to be straight-chain upon coordination to a metal, but so far that has not been observed. In fact, there are no reports of coordination complexes prepared by reacting metal salts with selenotelluride solutions, nor have our own efforts in that direction been successful. Reactions with phosphine tellurides, such as those described here, presently provide the only known route to selenotellurometalates.

**Acknowledgment.** This research was funded by the National Science Foundation, Grant No. CHE92-24469.

**Supplementary Material Available:** Experimental details (Tables S1, S5, and S9), atomic parameters (Tables S2, S6, and S10), anisotropic displacement parameters (Tables S3, S7, and S11), and bond distances and angles (Tables S4, S8, and S12) (49 pages). Ordering information is given on any current masthead page.

(28) Zagler, R.; Eisenmann, B. *Z. Kristallogr.* **1988**, *183*, 193–200.